

2-2012

Cardiomyopathy Detection from Electrocardiogram Features

Mirela Ovreiu

Cleveland Clinic Foundation, ovreium@ccf.org

Daniel J. Simon

Cleveland State University, d.j.simon@csuohio.edu

Follow this and additional works at: https://engagedscholarship.csuohio.edu/enece_facpub

 Part of the [Electrical and Computer Engineering Commons](#)

How does access to this work benefit you? Let us know!

Original Citation

M. Ovreiu and D. Simon, "Cardiomyopathy Detection from Electrocardiogram Features," in *Cardiomyopathies – From Basic Research to Clinical Management* (J. Veselka, editor) InTech, pp. 117–134, 2012

Repository Citation

Ovreiu, Mirela and Simon, Daniel J., "Cardiomyopathy Detection from Electrocardiogram Features" (2012). *Electrical Engineering and Computer Science Faculty Publications*. 142.
https://engagedscholarship.csuohio.edu/enece_facpub/142

This Contribution to Books is brought to you for free and open access by the Electrical and Computer Engineering Department at EngagedScholarship@CSU. It has been accepted for inclusion in Electrical Engineering and Computer Science Faculty Publications by an authorized administrator of EngagedScholarship@CSU. For more information, please contact library.es@csuohio.edu.

Cardiomyopathy Detection from Electrocardiogram Features

Mirela Ovreiu and Dan Simon

*Cleveland Clinic Foundation, Cleveland State University
United States*

1. Introduction

Cardiomyopathy refers to diseases of the heart muscle that becomes enlarged, thick, or rigid. These changes affect the electrical stability of the myocardial cells, which predisposes the heart to failure or arrhythmias. Cardiomyopathy in its two common forms, dilated and hypertrophic, implies enlargement of the atria. Therefore, computer intelligence techniques are proposed for the recognition and classification of P wave features for cardiomyopathy diagnosis. The technique that we propose is a neuro-fuzzy network. The neuro-fuzzy classifier will be trained with innovative evolutionary algorithms, which have recently been shown to be efficient global optimizers.

Cardiomyopathy is a significant clinical problem which is mainly generated by volume/diastolic overload. To accommodate the increased blood volume, the heart chambers may stretch or dilate. Valvular regurgitation and congestive heart failure are two conditions that contribute to chamber dilation.

Cardiomyopathy is generally diagnosed by an electrocardiographic (ECG) investigation. In the current standards published by the American Heart Association, chamber hypertrophy or enlargement is a separate diagnostic category which can be detected with ECG analysis (Masson, Hancock, & Gettes, 2007). Although many algorithms have been implemented for ECG analysis, the proposed research is unique in several ways.

- We propose the development of **non-invasive** and **automatic cardiomyopathy diagnosis**, which has not been reported in the literature.
- We propose the development of algorithms for **P wave analysis**, which have not been reported in the literature.
- We propose the use of **5-lead ECG data**, which is more readily available than 12-lead data.
- We propose the use of a powerful **neuro-fuzzy architecture** for ECG analysis, which has not been reported in the literature.
- We propose neuro-fuzzy ECG classifier optimization using **evolutionary algorithms**, which has not been reported in the literature.

Our preliminary studies of postoperative cardiovascular patients reveal our hypothesis: the ECG presents different electrical activity for patients with cardiomyopathy, compared with patients who do not have cardiomyopathy. This working hypothesis indicates that an automated method that selects the best ECG parameters to include in a cardiomyopathy

diagnosis algorithm will be extremely valuable. Although such a method will not be fool-proof or 100% correct, and thus cannot replace medical doctors, it will help physicians diagnose or prognose life threatening conditions such as stroke or ventricular or atrial fibrillation. This will expedite the initiation of medical treatment as appropriate to minimize the risk of these conditions, or to prevent their onsets.

Although it has long been suggested that cardiomyopathy is reflected in modification of ECG characteristics, statistics-based attempts to classify cardiomyopathy from the ECG have been underwhelming (Macfarlane, 2006; Magdic, Saul, 1997). Motivated by the universal approximation theorem for neuro-fuzzy networks discussed in the chapter, we hypothesize that earlier limitations may be overcome by a neuro-fuzzy classification model.

Cardiovascular diseases are the major cause of death in the western world, resulting in more than 800,000 deaths per year in the United States alone (American Heart Association, 2009). One in five Americans has some form of cardiovascular disease (Olson, 2004).

Cardiomyopathy is a significant clinical problem which is mainly generated by volume/diastolic overload. To accommodate the increased volume of blood, the heart chambers may stretch or dilate. Valvular regurgitation and congestive heart failure are two conditions that contribute to chamber dilation.

Cardiomyopathy is generally diagnosed by an echocardiograph investigation. For an echocardiography the patient has to be referred to a cardiologist or an echocardiographic investigation. But the electrocardiographic (ECG) investigation is always part of a cardiologic work-up.

The ECG represents the recording of the deflection of ionic current across myocardial cell membranes and throughout the extracellular space of the different tissues of the thoracic cavity. The ECG, in competition to many other techniques, retains an important role in diagnosis and prognosis of cardiovascular diseases.

It has been suggested that cardiomyopathy is reflected in modification of ECG characteristics such as P wave morphology. Previous statistics-based attempts to classify the cardiomyopathy from ECG have been underwhelming (Macfarlane, 2006; Magdic, Saul, 1997), but we hypothesize that these limitations can be overcome using a hybrid neuro-fuzzy classification model. To test this hypothesis and direct the results to patient care, we follow these directions. First we design a neuro-fuzzy model to diagnose cardiomyopathy. Then we train the network using an acquired clinical database of ECG signals.

Neuro-fuzzy systems can be trained with derivative-based methods like gradient descent (Chen, Linkens, 2001; Linkens, Chen, 1999) or with evolutionary algorithms such as genetic algorithms and swarm intelligence (Kennedy, Eberhart, & Shi, 2001). Evolutionary algorithms have the advantage of not requiring derivative information, and have less likelihood of getting stuck in a local optimum. Hence we use a new biologically motivated optimization algorithm called biogeography-based optimization (BBO) (Simon, 2008) to train the neuro-fuzzy ECG classification network. We also incorporate opposition-based learning in the BBO algorithm (Ergezer, Simon, & Du, 2009) for better classification.

2. Background

2.1 Cardiomyopathy

The term “cardiomyopathy” defines a group of diseases primarily affecting the cardiac muscle by weakening it or changing its structure. Cardiomyopathy can be acquired or inherited, and in many cases its cause is unknown. Hypertrophic cardiomyopathy is

inherited and is supposed to be a result of defects of genes that regulate heart muscle growth. Abnormal cardiac enlargement can be due to an increase in length or diameter of existing cardiac muscle cells (Olson, 2004). Cardiomyopathy, through electrical instability of myocardial cells, is associated with cardiac conduction abnormalities that can degenerate to arrhythmia or heart failure (Dische, 1972).

Cardiomyopathies, especially hypertrophic, are considered a common cause of sudden cardiac death in young adults and children (Ingles, Semsarian, 2007; Bar-Cohen, Silka, 2008). The Chagas and idiopathic dilated etiologies of cardiomyopathy led to Pereira et al.'s study in adults (Pereira et al., 2010); after 40 months, almost half of the cases studied (113 out of 284) registered deaths (104) or heart transplants (9).

The ECG records the deflection of ionic current across myocardial cell membranes and through the extracellular space of the thoracic cavity tissues. The history of cardiomyopathy research reveals the evolution of the analysis of ECG correlations. Due to the left ventricle's critical role, initial studies were focused only on the ECG features of the hypertrophic left ventricle (Sox, Garber, Littenberg, 1989). The QRS and T waves, as the reflections of ventricular depolarization and repolarization respectively, were analyzed (Ziegler, 1970). In the study by Sox et al., citing the Framingham Study, the left ventricular hypertrophy (LVH) was defined by a prolonged ventricular activation period of 0.05 s, tall R waves, depressed ST segments, and inverted T waves (Sox, Garber, Littenberg, 1989). Ziegler was the first to analyze T waves related to LVH; he presented different patterns of the QRS and T configurations into left or right precordial limb leads (Ziegler, 1970). The P wave portrays atrial electrical activity, so changes in the atrial action potential and substrate are reflected in P wave timing or morphology (Chandy, 2004). Bahl et al. presented the P wave changes associated with the type and stage of the disease (Bahl, 1972). Analyzing the four chamber enlargements, Johnson et al. presented P wave changes for enlarged left and right atria (Johnson, Horan, & Flowers, 1977).

The atria, characterized by thin walls, respond to volume and pressure overload due to dilatation. Moreover, the enlargement of the associated ventricle is recognized as the cause of the enlargement of the atrium (Macfarlane, 2006; Magdic, Saul, 1997). The right atrium enlargement is recognized by the increased amplitude of the P wave (0.25 mV) while left atrial abnormality is reflected by the lengthened P wave duration (>120 ms) as well as a notched P wave.

The American Heart Association, American College of Cardiology Foundation, and the Heart Rhythm Society, recently concluded on standards to be used when interpreting ECG data related to cardiomyopathy (Hancock et al., 2009). In left ventricular hypertrophy, the P wave shape is mentioned as a criterion. In right ventricular hypertrophy (LVH), a P wave amplitude larger than 0.25 mV in lead II is presented as a threshold. Left atrial abnormality implies a prolongation of the total atrial activation time (>120 ms), widely notched P wave, and possible changes in P wave area. The right atrial abnormality list includes a larger amplitude of the P wave (> 0.25 mV) and a prolongation of the P wave in patients after cardiac surgery, which is the case for the patients in our proposed research.

Our proposed algorithm presents the advantage of compatibility with the clinical Cardio-Vascular Intensive Care Unit (CVICU) setting since it is designed to analyze P wave parameters from a 5-lead ECG, versus the laboratory 12-lead ECG. P wave delineation is made automatically on the ECG signal using wavelet transforms. The P wave features obtained by the wavelets are then processed by a neuro-fuzzy system. Neuro-fuzzy systems are

combinations of fuzzy systems and artificial neural networks. Such combined systems have the advantage that they can learn faster and more accurately than an individual artificial neural network or fuzzy logic system. A benefit over artificial neural networks is that the rules that describe the system are explicit, thus permitting easy interpretation and validation.

Considering the frequent association of cardiomyopathy and atrial fibrillation, a future application of this successful classification process is the inclusion of the results in an automatic prediction algorithm for atrial fibrillation (AF). AF is a threatening arrhythmia that is encountered in 25% of post-cardiovascular surgical patients in the CVICU of the Cleveland Clinic.

Cardiomyopathy diagnosis will be performed by a multivariate, neuro-fuzzy classification model that uses P wave parameters to generate a cardiomyopathy classification index. Artificial Neural Networks are universal approximators (Buckley, Hayashi, 1995), and there has also been extensive work to prove that neuro-fuzzy systems can approximate any continuous function to any desired degree of accuracy (Feuring, Lippe, 1999). Alvisi et al. (Alvisi et al., 2006) have studied the performances of fuzzy logic and Artificial Neural Networks, revealing the weaknesses and strengths of each of the methods. The strengths can be emphasized, and some of the weaknesses can be attenuated, by combining the techniques into a hybrid neuro-fuzzy model. **The universal approximation theorem is the reason that a neuro-fuzzy system may be able to overcome the limitations of previous statistics-based methods for ECG analysis.**

2.2 Neuro-fuzzy networks

Consider a multi-input, single-output fuzzy logic system. Our discussion can be easily generalized to multiple output systems, but restricting our discussion to single-output systems simplifies the notation considerably. In addition, the ECG classification system that we consider in this paper is single-output. The i th rule R_i of the fuzzy system can be written as follows (Chen, Linkens, 2001).

$$R_i : \text{If } x_1 \text{ is } A_{i1} \text{ and } \dots \text{ and } x_m \text{ is } A_{im} \text{ then} \\ y = z_i(x), \quad (i = 1, \dots, p). \quad (1)$$

The inputs x_i and the output y are linguistic variables, A_{ij} are fuzzy sets, and $z_i(x)$ is a function of the input $x = [x_1 \dots x_m]^T$. The output function $z_i(x)$ typically takes one of the following forms: (1) singleton, (2) fuzzy set, (3) linear function. If the fuzzy system uses center average defuzzification, product inference, and singleton fuzzification, then $z_i(x) = z_i$ (a singleton) and the fuzzy system output can be written as

$$y = \frac{\sum_{i=1}^p z_i \prod_{j=1}^m \mu_{ij}(x_j)}{\sum_{i=1}^p \prod_{j=1}^m \mu_{ij}(x_j)} \quad (2)$$

where $\mu_{ij}(x_j)$ denotes the degree of membership of x_j in R_i . As in many neuro-fuzzy networks, we use a Gaussian form for μ_{ij} :

$$\mu_{ij}(x_j) = \exp\left(-\frac{(x_j - c_{ij})^2}{\sigma_{ij}^2}\right) \quad (3)$$

where c_{ij} is the j th element of the center of the i th rule, and σ_{ij} is its standard deviation. In this case, Eq. (2) becomes

$$y = \frac{w}{\sum_{i=1}^p m_i(x)} \quad (4)$$

$$w = \sum_{i=1}^p z_i m_i(x) \quad (5)$$

$$m_i(x) = \exp[-(x - c_i)^T P^{-2}(x - c_i)] \quad (6)$$

where $c_i = [c_{i1} \cdots c_{im}]^T$ and $P = \text{diag}(\sigma_1, \cdots, \sigma_m)$. Eq. (5) is in the form of a radial basis function, which is a type of neural network (Chen, Linkens, 2001). The system of Eqs. (5) and (6) is therefore called a neuro-fuzzy system. It can be depicted as shown in Figure 1.

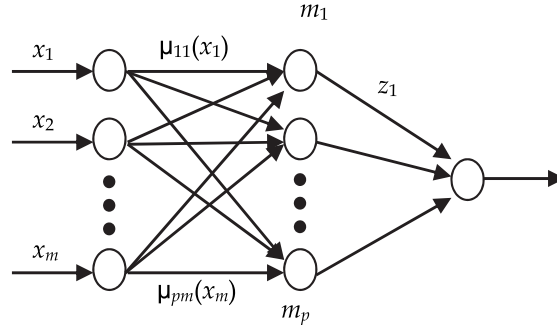


Fig. 1. Multi-input single-output neuro-fuzzy system architecture

The neuro-fuzzy system in Figure 1 is a function of the $p \times m$ elements of the membership centers c_{ij} , the $p \times m$ elements of the membership standard deviations σ_{ij} , and the p elements of the singleton outputs z_i . There are thus $p(2m+1)$ parameters that define the neuro-fuzzy system. For a given neuro-fuzzy system architecture and a given training set of input/output data, the neuro-fuzzy system parameters can be optimized with respect to these $p(2m+1)$ parameters.

2.3 Biogeography-Based Optimization (BBO)

Biogeography-based optimization (BBO) is a recently-developed population-based evolutionary optimization algorithm (Simon, 2008). As its name implies, BBO is motivated by biogeography, which is the study of the distribution of species over time and space (Whittaker, 1998). BBO has demonstrated good performance on various benchmark functions (Lomolino, Riddle, & Brown, 2009; Simon, 2008). It has also been successfully applied to several real-world optimization problems, including sensor selection (Simon, 2008), power system optimization (Rarick et al., 2009), groundwater detection (Kundra, Kaur, & Panchal, 2009), and satellite image classification (Panchal et al., 2009).

Given an optimization problem and a population of candidate solutions (individuals), a biogeography-based optimization (BBO) solution with high fitness is likely to share its features with other solutions, and a solution with low fitness is unlikely to share its features. Conversely, a solution with high fitness is unlikely to accept features from other solutions, while a solution low fitness is likely to accept features. Solution feature sharing, which is called immigration and emigration, tends to improve the solutions and thus evolve a good solution to the problem.

In biogeography-based optimization (BBO), each individual solution has its own immigration rate λ_i and emigration rate μ_i . A good solution has relatively high μ and low λ , while the converse is true for a poor solution. The immigration rate and the emigration rate are functions of the fitness of the solution. They are often calculated as

$$\begin{aligned}\lambda_i &= f_i/n \\ \mu_i &= 1 - \lambda_i\end{aligned}\tag{7}$$

where n is the population size and f_i is the fitness rank of the i th individual (the most fit individual has a rank $f_i = 1$). The immigration rates λ_i are interpreted by the BBO algorithm as immigration probabilities. The emigration rates μ_i are proportional to fitness and so are used in a roulette-wheel type of algorithm to determine the emigrating solution in case immigration is selected for a solution.

Although the migration rates in Eq. (1) are linear with respect to fitness rank as originally proposed in earlier study (Simon, 2008), more natural migration rates which are sigmoid with respect to fitness rank generally seem to give better optimization performance (Lomolino, Riddle, & Brown, 2009). However, in this paper we retain the original linear migration rates for the simplicity reason.

As with other evolutionary algorithms, mutation is typically implemented to increase exploration, and elitism is often implemented to retain highly fit solutions. The standard BBO algorithm is shown in Figure 2.

```

For each solution  $H_i$ 
  For each solution feature  $s$ 
    Select solution  $H_i$  with probability proportional to  $\lambda_i$ 
    If solution  $H_i$  is selected then
      Select  $H_j$  with probability proportional to  $\mu_j$ 
      If  $H_j$  is selected then
         $H_i(s) \leftarrow H_j(s)$ 
      end
    end
  end
  next solution feature
  Probabilistically mutate  $H_i$ 
next solution

```

Fig. 2. One generation of the standard BBO algorithm.

2.4 Oppositional BBO

Opposition-based learning (OBL) has been introduced as a method that can be used by Evolutionary Algorithms (EAs) to accelerate convergence speed by comparing the fitness of an individual to its opposite and retaining the fitter one in the population (Rahnamayan, Tizhoosh, & Salama, 2007; Tizhoosh, 2005). The “opposite” of an individual is defined as the reflection of that individual’s features across the midpoint of the search space. Opposition-based differential evolution (ODE) (Rahnamayan, Tizhoosh, & Salama, 2008.) was the first application of OBL to Evolutionary Algorithms (EAs). OBL was first incorporated in BBO in earlier research study (Ergezer, Simon, & Du, 2009) and was shown to improve BBO by a significant amount on standard optimization benchmarks.

Given an Evolutionary Algorithm (EA) population member x , there are at least three different types of oppositional points that can be defined. These oppositional points are referred to as the opposite x_o , the quasi-opposite x_q , and the quasi-reflected-opposite x_r . Figure 3 illustrates these points for an arbitrary x in a one-dimensional domain. The point c is the center of the domain, x_o the reflection of x across c , x_q is a randomly generated point from a uniform distribution between c and x_o , and x_r is a randomly generated point from a uniform distribution between x and c .

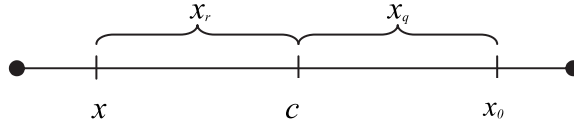


Fig. 3. Illustration of an arbitrary EA individual x , its opposite x_o , its quasi-opposite x_q , and its quasi-reflected-opposite x_r , in a one-dimensional domain.

OBL is essentially a more intelligent way of implementing exploration instead of generating random mutations. Another way of viewing OBL is from the perspective of social revolutions in human society. Society often progresses on the basis of a few individuals who embrace philosophies that are not just random, but that are deliberately contrary to accepted norms. Given that an EA individual is described by the vector x , and that the solution to the optimization problem is uniformly distributed in the search domain, it is shown in Rahnamayan’s study (Rahnamayan, Tizhoosh, Salama, 2007) that x_q is probably closer to the solution than x or x_o . Further, it is presented in our earlier publication (Ergezer, Simon, & Du, 2009) that x_r is probably closer to the solution than x_q . These results are nonintuitive, but results related to random numbers are often nonintuitive, and the OBL results are derived not only analytically but also using simulation.

In this paper we use oppositional BBO (OBBO) to train the neuro-fuzzy ECG classification network. Suppose that the population size is N . OBBO works by generating a population of N opposite individuals which are the opposite of the current population. Then, given the entire $2N$ individuals comprised of both the original and the opposite populations, the best N individuals are retained for the next population. However, this does not occur at each generation. Instead it occurs randomly with a probability of J_r at each generation. J_r is called the jump rate. Based on (Rahnamayan, Tizhoosh, & Salama, 2006) we use $J_r = 0.3$ in this paper.

In order to increase the likelihood of improvement at each generation we implement OBBO as follows. At each generation, we save the original population of N individuals before

creating a population of N new individuals via migration. We then create an opposite population of N additional individuals if indicated by the jump rate. Of the total $2N$ or $3N$ individuals, we finally select the best N for the next generation. Note that this approach guarantees that the best individual in each generation is at least as good as that of the previous generation. This is similar to a $(\mu+\lambda)$ evolutionary strategy (Du, Simon, & Ergezer, 2009), whose parameters are not to be confused with the μ and λ migration parameters in BBO. The resulting OBBO algorithm is summarized in Figure 4.

```

 $H^{(1)} \leftarrow H$  (make a copy of the population  $H$ )
For each solution  $H_i \in H^{(1)}$  ( $i = 1, \dots, N$ )
  For each solution feature  $s$ 
    Select solution  $H_i$  with probability proportional to  $\lambda_i$ 
    If solution  $H_i$  is selected then
      Select  $H_j$  with probability proportional to  $\mu_j$ 
      If  $H_j$  is selected then
         $H_i(s) \leftarrow H_j^{(1)}$ 
      end
    end
  end
  Probabilistically mutate  $H_i$ 
next solution
if  $\text{rand}(0,1) < J$ , then
  Use  $H$  to create an  $N$ -member opposite population  $H^{(2)}$ 
else
   $H^{(2)} = \emptyset$ 
end
Copy the best  $N$  individuals from  $\{H, H^{(1)}, H^{(2)}\}$  to  $H$ 

```

Fig. 4. One generation of oppositional BBO (OBBO).

3. ECG data

In preparation for the testing of a cardiomyopathy diagnosis model, a database of long-duration ECG signals was collected. The database includes signals from 55 subjects, 18 of them with cardiomyopathy. Not all subjects experienced chronic or paroxysmal atrial fibrillation. The cardiomyopathy group contained 10 males and 8 females with a mean age of 54 (range 23–88) years. The control group contained 22 males and 15 females with a mean age of 60 (range 27–77) yrs. The inclusion criteria were the same for both groups: no chronic or paroxysmal atrial fibrillation and no perioperative pacing.

ECG parameters describing P wave morphology were computed for each minute of data recording for all 55 patients in the training data set. This set of ECG parameter values constitutes the input component of the training data set for neuro-fuzzy model development. For additional details of ECG parameter computation algorithms see (Bashour et al., 2004; Visinescu et al., 2004; Visinescu, 2005; Visinescu et al., 2006; Ovreiu et al., 2008)

The P wave from the electrocardiogram reflects the electrical activity of the atria and may indicate the existence of irregularities in electrical conduction. Using a previously developed P wave detection method, the starting, ending, and maximum points of the P wave were determined (Visinescu, 2005). The average P wave morphology parameters were computed once per minute. The P wave morphology parameters included the following:

- Duration
- Amplitude
- A shape parameter which represents monophasicity or biphasicity
- Inflection point, which is the duration of the P wave between the onset and the peak points
- Energy ratio, defined as the fraction between the right atrial excitation energy and the total atrial excitation energy.

Initial investigation revealed that the monophasicity / biphasicity parameter did not vary appreciably between cardiomyopathy and control patients. We therefore discarded the monophasicity / biphasicity parameter from our data set. Differences between the remaining P wave morphology parameters for cardiomyopathy and control patients in the training database are presented in Figure 5. Based on the standard deviation bars, there is apparently important information included in these parameters. Their usefulness in identifying the patients with cardiomyopathy is determined by the proposed neuro-fuzzy model as discussed in the following section.

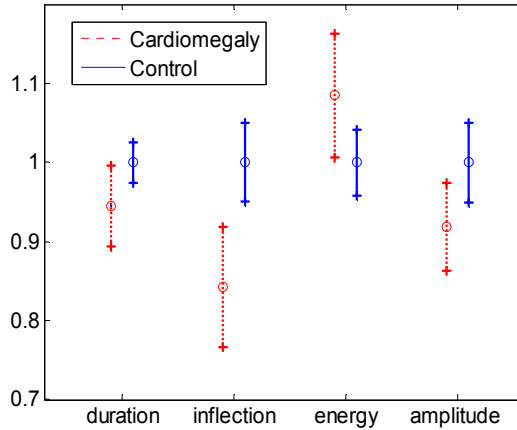


Fig. 5. P wave characteristics of cardiomyopathy and control patients. Data are normalized to the mean values of the control patients. Error bars show one standard deviation.

4. Experimental results

4.1 Problem setup

Cardiomyopathy diagnosis is performed by a multivariate, neuro-fuzzy classification model that uses current values of ECG P wave parameters to generate a cardiomyopathy classification index. The initial model is a multi-input single-output fuzzy inference system with a three-layer architecture (Figure 1). The fuzzification layer takes crisp parameter values and determines their memberships in linguistic categories (low, medium, high, etc.).

Each of these fuzzy variables are then input to each node of the fuzzy rule layer (i.e., the middle layer shown in Figure 1). The model output, which is the cardiomyopathy classification index, is the weighted average of the output rules.

Since we have four inputs (see Figure 5), we have $m = 4$ in Figure 1. The number of middle-layer neurons is equal to p and should be chosen as a tradeoff between good training performance and good generalization. If p is too small then training performance will be poor because we will not have enough degrees of freedom in the neuro-fuzzy network. If p is too large then test performance will be poor because the training algorithm will tend to “memorize” the training inputs rather than obtaining a good generalization for test data.

The output y shown in Eq. (4) is chosen to be +1 for cardiomyopathy patients and -1 for control patients. The ECG database is used for training and the output of the neuro-fuzzy system is compared to the known classification of the ECG patient. The RMS training error is defined as

$$E = \sqrt{\frac{1}{N} \sum_{i=1}^N (d_i - y_i)^2} \quad (8)$$

where N is the number of training inputs, d_i is the desired output of the i th training datum (+1 or -1), and y_i is the corresponding neuro-fuzzy output. In order to determine the best value of p (the number of middle-layer neurons) we run 10 Monte Carlo simulations with various values for p and compare training and testing errors. The BBO parameters that we use are as follows:

- Population size = 200
- Mutation rate = 2% per solution feature
- Generation limit = 50

Mutation is implemented by randomly generating a new parameter from a uniform distribution between the minimum and maximum parameter bounds. The parameter bounds that we use are as follows:

- Output singletons $z_i \in [-10, +10]$
- Membership centroids $c_{ij} \in [0, \pi]$
- Membership standard deviations $\sigma_{ij} \in [0.01, 5]$

We use ECG data from 55 test subjects as described in Section 3, which includes 37 control patients and 18 cardiomyopathy patients. We randomly divide the patients into approximately equal numbers of training patients and test patients. We therefore have 9 cardiomyopathy patients and 19 control patients for training the network, and 9 cardiomyopathy patients and 18 control patients for testing the network. We randomly choose 200 ECG data points from a 700-minute time interval for each patient for both training and testing. Therefore, we have $200 \times (9+19) = 5600$ data points for training, and $200 \times (9+18) = 5400$ data points for testing.

4.2 Parameter tuning and results

Table 1 shows the minimum training error attained as specified in Eq. (2) for various numbers of middle-layer neurons, along with the resulting correct classification rate for

training and testing. An ECG data point is classified as cardiomyopathy if the neuro-fuzzy output $y > 0$, and control if the neuro-fuzzy output $y < 0$. The quantity of primary interest is the correct classification rate for the test data, and Table 1 shows that this is attained with 3 middle-layer neurons. Fewer neurons gives too few degrees of freedom, and more neurons results in a tendency of the neuro-fuzzy system to overfit the training data and hence not provide adequate generalization for the test data.

| P | Training Error | | Train CCR (%) | | Test CCR (%) | |
|---|----------------|-------------|---------------|-----------|--------------|-----------|
| | Best | Mean | Best | Mean | Best | Mean |
| 2 | 0.85 | 0.88 | 76 | 72 | 66 | 58 |
| 3 | 0.77 | 0.84 | 82 | 77 | 75 | 62 |
| 4 | 0.78 | 0.83 | 84 | 77 | 65 | 55 |
| 5 | 0.78 | 0.83 | 82 | 76 | 63 | 58 |

Table 1. Training error and correct classification rate (CCR) for training and testing as a function of the number of middle layer neurons p .

Next we implement OBBO to explore the effect of OBL on classification performance. Table 2 shows results for three different OBL options: standard BBO, OBBO using quasi-opposition (Q-BBO), and OBBO using quasi-reflected opposition (R-BBO). We use the same population size, mutation rate, and generation limit as discussed earlier. We use 3 middle-layer neurons as indicated by Table 1. Table 2 shows that OBBO using quasi-opposition provides the best neuro-fuzzy classification performance when test performance is used as the criterion.

Note that the numbers in Tables 1 and 2 do not match exactly because they are the results of different sets of Monte Carlo simulations. In future work we will use a more extensive set of simulations in order to obtain results with a smaller margin of error.

| | Training Error | | Train CCR (%) | | Test CCR (%) | |
|--------------|----------------|-------------|---------------|-----------|--------------|-----------|
| | Best | Mean | Best | Mean | Best | Mean |
| BBO | 0.77 | 0.86 | 84 | 76 | 66 | 58 |
| Q-BBO | 0.83 | 0.86 | 79 | 74 | 69 | 62 |
| R-BBO | 0.80 | 0.85 | 81 | 75 | 65 | 60 |

Table 2. Training error and correct classification rate (CCR) for training and testing for alternative implementations oppositional BBO.

After settling on Q-BBO with 3 middle-layer neurons, we explore the effect of mutation rate on Q-BBO performance. Table 3 shows neuro-fuzzy results for various mutation rates. We use the same population size and generation limit as before. Table 3 shows that mutation rate does not have a strong effect on neuro-fuzzy system results, but based on test data performance, a low mutation rate generally gives better results than a high mutation rate.

| Mutation rate (%) | Training Error | | Train CCR (%) | | Test CCR (%) | |
|----------------------|----------------|-------------|---------------|-----------|--------------|-----------|
| | Best | Mean | Best | Mean | Best | Mean |
| 0.1 | 0.79 | 0.85 | 81 | 76 | 71 | 61 |
| 0.2 | 0.82 | 0.86 | 80 | 75 | 72 | 59 |
| 0.5 | 0.77 | 0.85 | 82 | 76 | 69 | 62 |
| 1.0 | 0.80 | 0.85 | 80 | 74 | 67 | 57 |
| 2.0 | 0.83 | 0.86 | 79 | 74 | 69 | 62 |
| 5.0 | 0.82 | 0.87 | 81 | 74 | 68 | 58 |
| 10.0 | 0.80 | 0.87 | 78 | 73 | 65 | 59 |

Table 3. Training error and correct classification rate (CCR) for different mutation rates using Q-BBO.

Figure 6 shows the progress for a typical Q-BBO training simulation. Note that the minimum training error in the top plot is monotonically nonincreasing due to the inherent elitism of the algorithm (see Figure 3). However, the average cost in the top plot, along with the success rates in the bottom plot, sometimes increases and sometimes decreases from one generation to the next. The results shown in Figure 6 also indicate that better results might be obtained if the generation limit were increased. However, care must be taken when increasing the generation limit. As the generation count increases, the training error will continue to decrease but the test error will eventually begin to increase due to overtraining (Tetko, Livingstone,& Luik, 1995).

The Q-BBO training run illustrated in Figure 6 resulted in the following neuro-fuzzy parameters:

$$c = \begin{bmatrix} 0.513 & 0.116 & 0.981 & 0.065 \\ 0.316 & 0.930 & 0.138 & 0.214 \\ 0.899 & 0.235 & 0.041 & 0.613 \end{bmatrix} \quad (9)$$

$$\sigma = \begin{bmatrix} 1.119 & 0.409 & 0.133 & 0.101 \\ 0.326 & 0.805 & 1.963 & 1.529 \\ 1.825 & 0.356 & 0.858 & 0.438 \end{bmatrix} \quad (10)$$

$$z = [1.641 \quad -0.967 \quad 0.779]. \quad (11)$$

Recall that we used a c range of $[0, \pi]$, but from Eq. (3) the highest membership centroid was less than 1 after Q-BBO training. This indicates that we could decrease the c range in order to get better resolution during training.

Similarly, recall that we used a σ range of $[0.01, 5]$, but from Eq. (4) the highest standard deviation was less than 2 after Q-BBO training. This indicates that we could decrease the σ range in order to get better resolution during training.

Finally, recall that we used an output singleton z range of $[-10, +10]$, but from Eq. (5) the output singletons were between -1 and 2 after Q-BBO training. This indicates that we could decrease the z range in order to get better resolution during training.

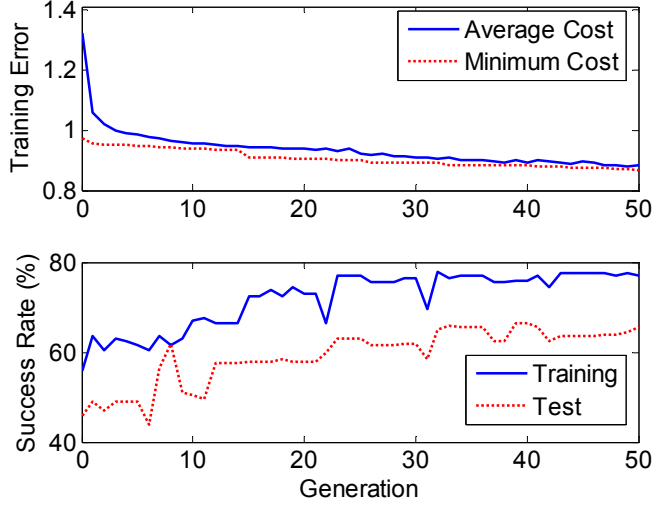


Fig. 6. Typical Q-BBO training results.

4.3 Clustering and pruning

The appropriate number of clusters in the neuro-fuzzy system is equivalent to the number of middle-layer neurons p shown in Figure 1. Determination of the optimal number of fuzzy rules is equivalent to finding a suitable number of clusters for the given data set. This can also be performed using fuzzy c-means clustering (Chen, Linkens, 2001; Linkens, Chen, 1999). Clustering is itself a multiobjective optimization problem that maximizes compactness within clusters, maximizes separation between clusters, and maximizes neuro-fuzzy system performance.

In the previous section we solved for cluster count using a direct approach involving manual tuning (see Table 1). However, we could also solve for cluster count by observing the output singletons z_i after training, discarding those that are significantly smaller than the others, and then retraining the network. This is a type of pruning. For example, when using BBO to train the neuro-fuzzy system with 5 middle-layer neurons, a typical result for the output singletons after convergence is

$$z = [1.766 \quad 1.880 \quad -1.712 \quad \mathbf{0.392} \quad -1.542].$$

It is seen that the magnitude of z_4 (0.392) is smaller by a factor of 4 than any of the other elements of z . This indicates that the corresponding fuzzy rule might be able to be safely removed from the neuro-fuzzy system without sacrificing performance. Retuning should then be performed because the neuro-fuzzy parameters will need to be adjusted to compensate for the network size reduction.

Another way to check if we are using too many middle-layer neurons is by looking at the distance between fuzzy membership function centers. If, after training, two membership function centers are very close to each other, that indicates that those two fuzzy sets could be combined. For example, the matrix of fuzzy centroids after a typical training run with 5 middle-layer neurons (i.e., 5 fuzzy membership sets) is given by

$$c = \begin{bmatrix} 0.5587 & 0.0046 & 0.9480 & 0.6628 \\ 0.4908 & 0.3719 & 0.4274 & 0.2847 \\ 0.5534 & 0.9005 & 0.9880 & 0.2659 \\ 0.9839 & 0.7428 & 0.3904 & 0.2067 \\ 0.9992 & 0.6061 & 0.2754 & 0.2185 \end{bmatrix}.$$

Each row of c corresponds to a fuzzy set centroid, and each column of c corresponds to one dimension of the input data. A cursory look at the c matrix shows that rows 4 and 5 are similar to each other. A matrix of Euclidean distances between centroids (i.e., between columns of c) can be derived as

$$\Delta c = \begin{bmatrix} 0 & 0.7439 & 0.9807 & 1.1157 & 1.0980 \\ 0.7439 & 0 & 0.7732 & 0.6231 & 0.5838 \\ 0.9807 & 0.7732 & 0 & 0.7556 & 0.8919 \\ 1.1157 & 0.6231 & 0.7556 & 0 & \mathbf{0.1797} \\ 1.0980 & 0.5838 & 0.7556 & \mathbf{0.1797} & 0 \end{bmatrix}$$

where Δc_{ij} is the Euclidean distance between centroids i and j . The Δc matrix indicates that fuzzy centroids 4 and 5 are much closer to each other than the other centroids, which implies that the corresponding membership functions overlap, and so they could be combined. Afterward, the neuro-fuzzy system should be retrained to compensate for the change in its structure.

4.4 Fine tuning using gradient information

The BBO algorithm that we used, like other Evolutionary Algorithms (EAs), does not depend on gradient information. Therein lies its strength relative to gradient-based optimization methods. Evolutionary Algorithms (EAs) can be used for global optimization since they do not rely on local gradient information. Since the neuro-fuzzy system shown in Figure 1 may have multiple optima, BBO training is less likely to get stuck in a local optima compared to gradient-based optimization.

However, additional performance improvement could be obtained in the neuro-fuzzy classifier by using gradient information in conjunction with EA-based optimization. Gradient-based methods can be combined with EAs in order to take advantage of the strengths of each method. First we can use BBO, as above, in order to find neuro-fuzzy parameters that are in the neighborhood of the global optimum. Then we can use a gradient-based method to fine tune the BBO result. The most commonly-used gradient-based method is gradient descent clustering (Chen, Linkens, 2001; Linkens, Chen, 1999). Gradient descent can be further improved by using an adaptive learning rate and momentum term (Nauck, Klawonn, Kruse, 1997).

Kalman filtering is a gradient-based method that can give better fuzzy system and neural network training results than gradient descent (Simon, 2002a, 2002b). Constrained Kalman filtering can further improve fuzzy system results by optimally constraining the network parameters (Simon, 2002c). H-infinity estimation is another gradient-based method that can be used for fuzzy system training to improve robustness to data errors (Simon, 2005).

4.5 Training criterion

The ultimate goal of the neuro-fuzzy network is to maximize correct classification percentage. If the neuro-fuzzy output is greater than 0, then the ECG is classified as cardiomyopathy;

otherwise, the ECG is classified as non-cardiomyopathy. The bottom plot in Figure 6 shows that while RMS training error is monotonically nondecreasing, the success rate for the training data is non-monotonic. We could more directly address the problem of ECG data classification by using classification success rate as our fitness function rather than trying to minimize the RMS error of Eq. (2). That is, in fact, one of the advantages of EA training relative to gradient-based methods – the fitness function does not have to be differentiable. However, if we use classification success rate as our fitness function, and then try to use a gradient-based method for fine-tuning, the cost functions of the two training methods would be inconsistent.

5. Conclusion

We have shown that clinical ECG data can be correctly classified as cardiomyopathy or non-cardiomyopathy using a neuro-fuzzy network training by biogeography-based optimization (BBO). Our results show a correct classification rate on test data of over 60%. Better results can undoubtedly be attained with further training, but the main goal of this initial research was to demonstrate feasibility and to establish a framework for further refinement.

Although our preliminary results are good, there are many enhancements that need to be made in order to improve performance and incorporate this work into a commercial product. For example, demographic information needs to be included with the ECG data. Some of the test ECGs were correctly classified 100% of the time, while others had a very low success rate. Figure 7 shows the classification success rate for the test data as a function of patient ID. Some patients generated ECG data that was successfully classified as cardiomyopathy / non-cardiomyopathy only 2% of the time, while others generated data that was successfully classified 100% of the time. This indicates that demographic data is important and that we should group patients into similar groups for testing and training. Some of these data include gender, race, medication usage, and age. This will become feasible as we perform more clinical studies and collect data from more patients.

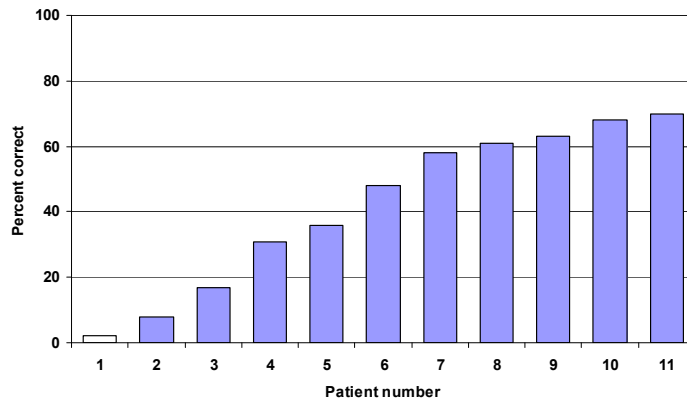


Fig. 7. ECG classification success rate for test patients.

We note that our results are based on snapshots of the data at single instants of time. We could presumably get better results by using a “majority rules” strategy for data collected over several minutes. For example, suppose that test accuracy is 60% for a given patient. We could use ECG data at three separate time instants and diagnose cardiomyopathy if the

neuro-fuzzy network predicts cardiomyopathy for two or more of the data. This would boost test accuracy from 60% to 65%, assuming that the probability of correct classification is independent from one time instant to the next. We could then further improve accuracy by using more time instants.

A strong reason for investigating this cardiac anomaly is its association to Atrial Fibrillation occurrence. The availability of ECG registrations and efficiency in time and cost savings of such a different approach, especially in cardiovascular surgical patients would imply as a future work, the inclusion of this automated classification algorithm into a bed side monitor indicator that might be used in future classification and/or forecasting algorithms under investigation.

6. Acknowledgement

This work was partially supported by Grant 0826124 in the CMMI Division of the Engineering Directorate of the National Science Foundation and Grant NCRP 10CRP2600305 from American Heart Association.

7. References

- Alvisi, S., Mascellani, G., Franchini, M., & Bardossy, A. (2006) – Water level forecasting through fuzzy logic and artificial neural network approaches, *Hydrology and Earth System Sciences*, 10 (1), pp. 1-17, 2006
- American Heart Association, (2009). *Heart Disease and Stroke Statistics – 2009 Update*, www.americanheart.org/presenter.jhtml?identifier=3018163
- Bahl, O. (1972) – Electrocardiographic and vectorcardiographic pattern in cardiomyopathy, *Cardiovascular Clinics*, 4 (1), pp. 95-112, 1972
- Bar-Cohen, Y., Silka, M. (2008) – Sudden cardiac death in pediatrics, *Current Opinion in Pediatrics*, 20 (5), pp. 517-521, 2008
- Bashour, C., Visinescu, M., Gopakumaran, B., Wazni, O., Carragio, F., Yared, J., & Starr, N. (2004). Characterization of premature atrial contraction activity prior to the onset of postoperative atrial fibrillation in cardiac surgery patients, *Chest*, 126, 4 (2004), 831S.
- Buckley, J. and Hayashi, Y. (1995) – Neural Nets for Fuzzy Systems, *Fuzzy Sets and Systems*, 71 (3), pp. 265-276, 1995
- Chandy, J., Nakai, T., Lee, R., Bellows, W., Dzankic, S., & Leung, J. (2004) – Increases in P-wave Dispersion Predict Postoperative Atrial Fibrillation After Coronary Artery Bypass Graft Surgery, *Anesthesia & Analgesia*, 98, pp. 303-310, 2004
- Chen, M. and Linkens, D. (2001). A systematic neuro-fuzzy modelling framework with application to material property prediction, *IEEE Transactions on Systems, Man, and Cybernetics – Part B: Cybernetics*, 31, 5 (2001), pp. 781-790.
- Dische, M. R. (1972) – Observations on the morphological changes of the developing heart. *Cardiovascular Clinics*, 4 (3), pp. 175-191, 1972
- Du, D., Simon, D., & Ergezer, M. (2009). Biogeography-based optimization combined with evolutionary strategy and immigration refusal. *In Proceedings of the IEEE Conference on Systems, Man, and Cybernetics (San Antonio, Texas, October 2009)*. pp. 1023–1028.
- Ergezer, M., Simon D., & Du, D. (2009). Oppositional biogeography-based optimization. *In Proceedings of the IEEE Conference on Systems, Man, and Cybernetics (San Antonio, Texas, October 2009)*. pp. 1035–1040.

-
- Feuring, T. and Lippe, W.-M. (1999) – The fuzzy neural network approximation lemma, *Fuzzy Sets and Systems*, 102 (2), pp. 227-236, 1999
- Hancock, E.W., Mirvis, D.M., Okin, P., et al (2009) – AHA/ACCF/HRS recommendations for the standardization of interpretation of the electrocardiogram: part V: electrocardiogram changes associated with cardiac chamber hypertrophy: a scientific statement from the American Heart Association, Council on Clinical Cardiology; The American College of Cardiology Foundation, and the Heart Rhythm Society, *Journal of American College of Cardiology*, 53: pp. 992-1002, 2009
- Heart Disease and Stroke Statistics*,
<http://www.americanheart.org/presenter.jhtml?identifier=3018163>, 2010
- Ingles, J, Semsarian, C (2007) – Sudden cardiac death in the young: A clinical genetic approach, *Internal Medicine Journal*, 37 (1), pp. 32-37, 2007
- Johnson, J. C., Horan, L. G., & Flowers, N. C. (1977) – Diagnostic accuracy of the electrocardiogram, *Cardiovascular Clinics*, 8 (3), pp. 25-40, 1977
- Kennedy, J., Eberhart, R., & Shi, Y. (2001). *Swarm Intelligence*. Morgan Kaufmann.
- Kundra, H., Kaur, A., & Panchal, V. (2009). An integrated approach to biogeography based optimization with case based reasoning for retrieving groundwater possibility. In *Proceedings of the 8th Annual Asian Conference and Exhibition on Geospatial Information, Technology and Applications (Singapore, August 2009)*.
- Linkens, D. and Chen, M. (1999). Input selection and partition validation for fuzzy modelling using neural network. *Fuzzy Sets and Systems*, 107, 3 (1999), pp. 299–308.
- Lomolino, M., Riddle, B., & Brown, J. (2009). *Biogeography*. Sinauer Associates.
- Macfarlane, P. W. (2006) – Is electrocardiography still useful in the diagnosis of cardiac chamber hypertrophy and dilatation?, *Cardiology Clinics*, 24 (3), pp. 401-411, 2006
- Magdic, K. S., Saul, L. M. (1997) – ECG Interpretation of chamber enlargement, *Critical Care Nurse*, 17 (1), 13, 16-25, 1997
- Masson, J. M., Hancock, E. W., & Gettes, L. S. (2007) – AHA/ACC/HRS Scientific Statement, Recommendations for Standardization and Interpretation of the Electrocardiogram. Part II: Electrocardiography Diagnostic Statement List, A Scientific Statement From the American Heart Association Electrocardiography and Arrhythmias Committee, Council on Clinical Cardiology; The American College of Cardiology Foundation, and the Heart Rhythm Society, *Circulation*. 115: pp. 1325-1332, 2007
- McKenna, W. J., Krikler, D. M., & Goodwin, J. F. (1982) – Arrhythmias in dilated and hypertrophic cardiomyopathy. *Medical Clinics of North America*, 68 (4), pp. 983-1000, 1984
- Nauck, D., Klawonn, F., and Kruse, R. (1997). *Foundations of Neuro-Fuzzy Systems*. John Wiley & Sons.
- Olson, E. N. (2004) – A decade of discoveries in cardiac biology, *Nature Medicine* 10, pp. 467-474, 2004
- Ovreiu, M., Nair, B., Xu, M., Bakri, M., Li, L., Wazni, O., Fahmy, T., Petre, J., Sessler, D., Starr, N., & Bashour, A. (2008) Electrocardiographic Activity Before Onset of Postoperative Atrial Fibrillation in Cardiac Surgery Patients, *PACE*, November 2008, Vol. 31, issue 11, pp. 1371-1382 (with editorial comment of Lombardi, F. (2008) – “Atrial Fibrillation After cardiac Surgery: Prevention or Early Treatment of Patients at Risk”, *PACE*, November 2008, Vol. 31, issue 11, pp. 1369-1370)
- Panchal, V., Singh, P., Kaur, N., & Kundra, H. (2009). Biogeography based satellite image classification. *International Journal of Computer Science and Information Security*. 6, 2 (Nov. 2009), pp. 269–274.

-
- Pereira, N., Barbosa, M., Ribeiro, A., Amorim, F., & Rocha, M. (2010) – Predictors of mortality in patients with dilated cardiomyopathy: Relevance of Chagas disease as an etiological factor, *Revista Espanola de Cardiologia*, 63 (7), pp. 788-797, 2010
- Rahnamayan, S., Tizhoosh, H., & Salama, M. (2006). Opposition-based differential evolution for optimization of noisy problems, in *Proceedings of IEEE Congress on Evolutionary Computation (Vancouver, Canada, July 2006)*. pp. 1865–1872.
- Rahnamayan, S., Tizhoosh, H., & Salama, M. (2007). Quasioppositional differential evolution, in *Proceedings of IEEE Congress on Evolutionary Computation (Singapore, September 2007)*. 2229–2236.
- Rahnamayan, S., Tizhoosh, H., & Salama, M. (2008). Opposition-based differential evolution. *IEEE Transactions on Evolutionary Computation*, 12, 1 (2008), pp. 64–79.
- Rarick, R., Simon, D., Villaseca, F. E., & Vyakaranam, B. (2009). Biogeography-based optimization and the solution of the power flow problem, In *Proceedings of the IEEE Conference on Systems, Man, and Cybernetics (San Antonio, Texas, October 2009)*. pp. 1029–1034.
- Simon, D. (2002a). Training fuzzy systems with the extended Kalman filter. *Fuzzy Sets and Systems*, 132, 2 (December 2002), pp. 189–199.
- Simon, D. (2002b). Training radial basis neural networks with the extended Kalman filter. *Neurocomputing*, 48, 1 (October 2002), pp. 455–475.
- Simon, D. (2002c). Sum normal optimization of fuzzy membership functions. *International Journal of Uncertainty, Fuzziness, and Knowledge-Based Systems*, 10, 4 (August 2002), pp. 363–384.
- Simon, D. (2005). H-infinity estimation for fuzzy membership function optimization, *International Journal of Approximate Reasoning*, 40, 3 (November 2005), pp. 224–242.
- Simon, D. (2008). Biogeography-Based Optimization, *IEEE Transactions on Evolutionary Computation*, 12, 6 (December 2008), pp. 702–713.
- Sox, H. C., Garber, A. M., & Littenberg, B. (1989). The resting Electrocardiogram as a Screening Test: A Clinical Analysis, *Annals of Internal Medicine*, 111, pp. 489-502, 1989
- Tetko, I., Livingstone, D., & Luik, A. (1995). Neural network studies. 1. Comparison of overfitting and overtraining. *Journal of Chemical Information and Modeling*, 35, 5 (September 1995), pp. 826–833.
- Tizhoosh, H. (2005). Opposition-based learning: A new scheme for machine intelligence, in *Proceedings of the International Conference on Computational Intelligence for Modelling, Control and Automation (Vienna, Austria, November 2005)*. pp. 695–701.
- Visinescu, M., Bashour, A., Wazni, O., & Gopakumaran, B. (2004). Automatic detection of conducted premature atrial contractions to predict atrial fibrillation in patients after cardiac surgery, in *Proceedings of the 31st Annual International Conference on Computing in Cardiology (Chicago, Illinois, September 2004)*. pp. 429–432.
- Visinescu, M. (2005). *Analysis of ECG to predict atrial fibrillation in post-operative cardiac surgical patients. Doctoral dissertation*, Cleveland State University, Cleveland, Ohio.
- Visinescu, M., Bashour, A., Bakri, M., & Nair, B. (2006). Automatic detection of QRS complexes in ECG signals collected from patients after cardiac surgery, in *Proceedings of the 28th Annual International Conference of the IEEE Engineering in Medicine and Biology Society (New York, August 2006)*. pp. 3724–3727.
- Ziegler, R. F. (1970). Electrocardiographic Clues in the diagnosis of congenital heart disease, *Cardiovascular Clinics*, 2 (1), pp. 97-114, 1970
- Whittaker, R. (1998). *Island Biogeography*. Oxford University Press.